

# Improved Switching Uniformity of a Carbon-based ReRAM device by Controlling Size of Conducting Filament

Jubong Park<sup>1</sup>, Hyejung Choi<sup>1</sup>, Minseok Jo<sup>1</sup>, Joonmyoung Lee<sup>1</sup>, Tae-Wook Kim<sup>1</sup>, Jaesik Yoon<sup>1,2</sup>, Dong-jun Seong<sup>1</sup>, Wootae Lee<sup>1</sup>, Man Chang<sup>1</sup>, Jungho Shin<sup>2</sup>, Takhee Lee<sup>1</sup>, and Hyunsang Hwang<sup>1,2</sup>

Department of Materials Science and Engineering, Gwangju Institute of Science and Technology<sup>1</sup>,  
Department of Nanobio Materials and Electronics<sup>2</sup>

261 Cheomdan-gwagiro (Oryong-dong), Buk-gu, Gwangju 500-712, Republic of Korea

Phone: +82-62-970-2314, Fax: +82-62-970-2304, e-mail: hwanghs@gist.ac.kr

## 1. Introduction

We investigated the resistive switching properties of a Carbon based ReRAM device. In order to minimize the fluctuations of switching parameters, we introduced an external load resistor ( $R_{Load}$ ) in series, which indirectly acts as a current limiter. Reduced reset current ( $I_{reset}$ ) and improved switching uniformity were obtained when the proper external  $R_{Load}$  was connected. The voltage drop at the ReRAM device during switching was directly monitored using an oscilloscope.

## 2. Experimentals

As a resistive memory, Cu/carbon/Pt structure resistive memory device was fabricated. The carbon layer was deposited onto a Pt substrate by RF magnetron sputtering at room temperature using a carbon target. Using scanning electron microscopy (SEM) analysis and transmission electron microscopy(TEM) diffraction pattern as shown in Fig. 1(a), we have confirmed a 30 nm-thick amorphous carbon layer as shown in Fig. 1(a). After conventional lithography process, a 100 nm-thick Cu top electrode with an area of  $30 \times 30 \mu m^2$  was formed via sputtering. A schematic diagram of the device structure is shown in inset of Fig. 1(b).

## 3. Results & Discussion

As shown in Fig. 1 (b), it shows bipolar switching characteristics by the motion of Cu ions. For further understanding about the switching mechanism, the double logarithm plot at set operation region is shown in Fig. 2 (a) which indicates the linear dependence of voltage and current with slope about one [1]. Moreover, we concluded the switching mechanism as the of filamentary theory based on the temperature variable analysis as shown Fig. 2 (b) which consistent with the fact that the resistance of metal is proportional to the temperature [2]. In pulse mode, excess current flowing during the set operation cannot be controlled by the measurement instrument. Because of the nonexistence of  $I_{comp}$  in pulse mode, the excess current forms a thick conductive filament and causes hard failure of the device [3]. To protect the device from excess current flow under pulse switching conditions, an  $R_{Load}$  was used to indirectly maintain  $I_{comp}$ . The device was connected to  $R_{Load}$  ( $=10 \text{ k}\Omega$ ) only during the set operation. Fig. 3 (a) shows the pulse switching characteristics. We have confirmed stable switching characteristics under pulse switching conditions by adding  $R_{Load}$ . To clearly understand the effect of  $R_{Load}$  on resistive switching, the switching parameters were monitored with varying  $R_{Load}$  under DC switching mode. As shown in Fig. 3(b), we found that  $I_{reset}$  is inversely

proportional to  $R_{CF}$ . High  $R_{CF}$  indicates a smaller-diameter conducting filament (CF), which in turn reduces  $I_{reset}$ . To control the size of CF, we intentionally added a series resistor ( $R_{Load}$ ). Fig. 3(c) shows the effect of  $R_{Load}$  on  $I_{reset}$ . With increasing resistance of  $R_{Load}$ ,  $I_{reset}$  was significantly reduced, indicating a smaller-diameter CF that requires less power to reset. Fig. 4 shows the retention properties at  $85^\circ\text{C}$  as a function of  $R_{CF}$ . We found degradation of retention characteristics, which can be explained by the smaller diameter of the CF and migration of copper ions.

Figs. 5(a) and (b) show the cumulative probability distribution of  $I_{reset}$ , set voltage ( $V_{set}$ ) and reset voltage ( $V_{reset}$ ). The average value of  $I_{reset}$  and the standard deviation of  $I_{reset}$ ,  $V_{set}$  and  $V_{reset}$  are summarized in Table 1. Significant improvement of switching uniformity was observed by connecting  $R_{Load}$ . To clearly understand the effect of  $R_{Load}$  on switching uniformity, we used an oscilloscope to directly measure the effective voltage across a ReRAM device during the set operation, as shown in Fig. 5(c). Relatively small fluctuation was observed when  $R_{Load}$  ( $=100 \text{ k}\Omega$ ) was connected. These behaviors might be related to the soft breakdown (SB) phenomena observed in gate dielectrics [4]. Therefore, the voltage fluctuation in Fig. 5(c) can be reduced by suppressing the movement of Cu ions, which are sensitive to applied voltage.

## 4. Summary

For high-density memory applications of ReRAM devices, improved switching uniformity and reduced switching power are required. To solve these problems, we introduced the external series resistor  $R_{Load}$ . A ReRAM device with  $R_{Load}$  shows improved switching characteristics that can be explained by formation of uniform conducting filament. By controlling  $R_{Load}$ , we can accurately adjust the size and resistance of the conducting filament.

## Acknowledgments

This work was supported by the national research program of the 0.1 Terabit Non-volatile Memory Development Project, the National Research Laboratory (NRL) Programs of the Korea Science and Engineering Foundation (KOSEF) and the World Class University (WCU) program at GIST through a grant provided by the Ministry of Education, Science and Technology (MEST) of Korea.

## References

- [1] M. Pyun et al., *Appl. Phys. Lett.*, **93** (2008) 212907
- [2] H. Choi et al., *IEEE Electron Device Letters*, **30** (2009) 302
- [3] Y. Sato et al., *IEEE Trans. Electron Devices*, **55** (2008) 1185
- [4] T. Tomita *IEEE Trans. Electron Devices*, **46** (1999) 159

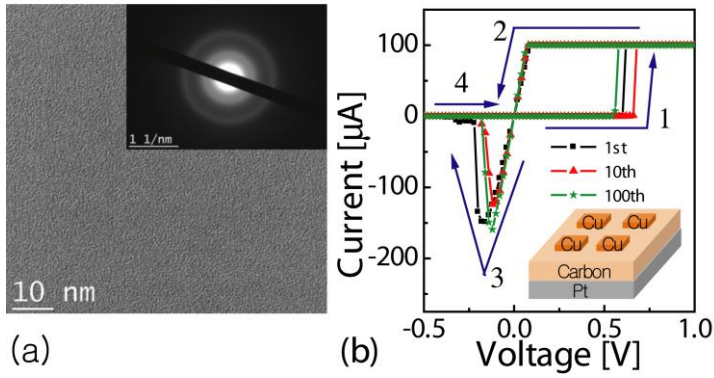


**Fig. 1** (a) The plan-view TEM image and the diffraction pattern of carbon layer. (b) I-V hysteresis of Cu/carbon/Pt device. The inset of figure shows the schematic diagram of Cu/Carbon/Pt structure.

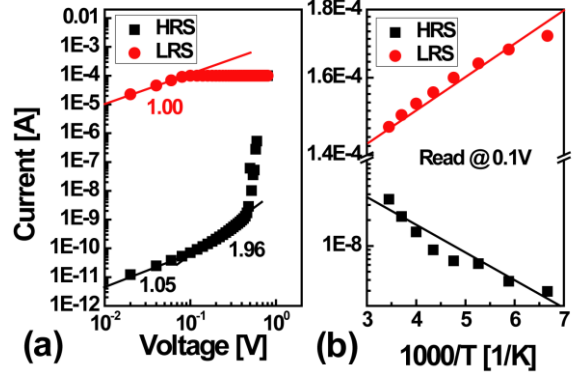


**Fig. 2** (a) The I-V characteristics in a double-logarithmic plot at the positive bias region. (b) The temperature variable I-V characteristics in range from 150K to 295K.

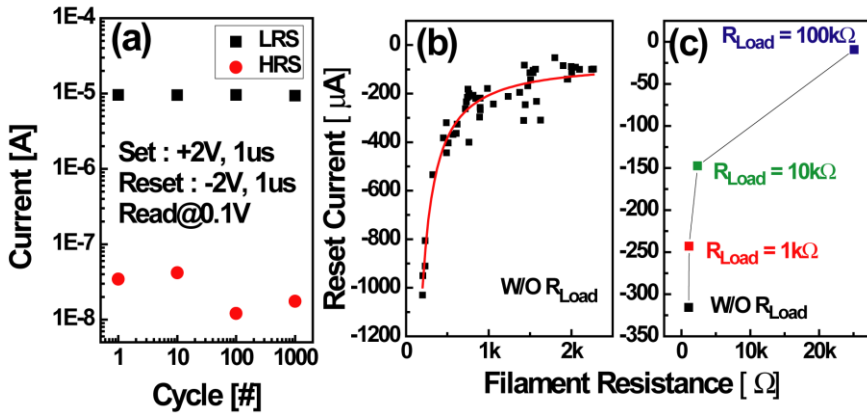


**Fig. 3** (a) Pulse switching properties and the pulse width dependence of the Cu/Carbon/Pt sample using a series resistor. (b) Dependence of reset current on the filament resistance. The data was obtained from fifty DC switching cycles in one spot. (c) The reduced reset current using a series resistor. As the connected resistance increased, the reset current was decreased.

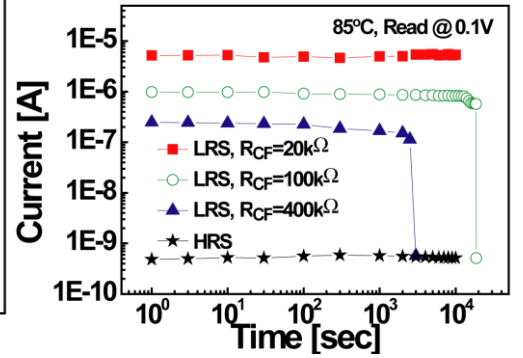


**Fig. 4** The retention properties at 85°C for 10<sup>4</sup> sec. The LRS was programmed using various resistors.

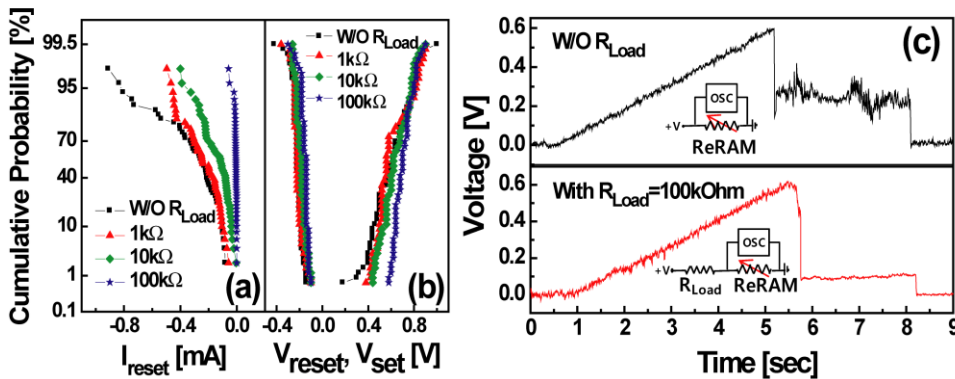


**Fig. 5** (a) The cumulative probability distribution of the reset current and (b) the set/reset voltage. As the connected resistance is increased, a narrower reset current and set/reset voltage distribution is observed. (c) The voltage fluctuation of the set operation with/without a load resistor in real-time measurements.

Table 1. The average value of  $I_{\text{reset}}$  and standard deviation of  $I_{\text{reset}}$ ,  $V_{\text{set}}$  and  $V_{\text{reset}}$

$R_{\text{Load}}$	AVG of $I_{\text{reset}}$	STD of $I_{\text{reset}}$	STD of $V_{\text{set}}$	STD of $V_{\text{reset}}$
0	-3.2E-4	2.3E-4	0.18	0.051
10	-2.4E-4	1.3E-4	0.16	0.047
10k	-1.5E-4	1.1E-4	0.13	0.046
100k	-9.3E-6	1.4E-5	0.08	0.042

<Table. 1>